J. Earth Syst. Sci. (2017) 126:97
DOI 10.1007/s12040-017-0862-7

Static elastic deformation in an orthotropic half-space with rigid boundary model due to non-uniform long strike slip fault

Yogita Godara[1,*], Ravinder Kumar Sahrawat[1] and Mahabir Singh[2]

[1] *Deenbandhu Chhotu Ram University of Science and Technology, Murthal, Sonepat 131 039, India.*
[2] *COE, Deenbandhu Chhotu Ram University of Science and Technology, Murthal, Sonepat 131 039, India.*
**Corresponding author. e-mail: anjali18feb2010@gmail.com*

MS received 25 January 2016; revised 2 February 2017; accepted 6 March 2017; published online 6 October 2017

The solution of static elastic deformation of a homogeneous, orthotropic elastic uniform half-space with rigid boundary due to a non-uniform slip along a vertical strike-slip fault of infinite length and finite width has been studied. The results obtained here are the generalisation of the results for an isotropic medium having rigid boundary in the sense that medium of the present work is orthotropic with rigid boundary which is more realistic than isotropic and the results for an isotropic case can be derived from our results. The variations of displacement with distance from the fault due to various slip profiles have been studied to examine the effect of anisotropy on the deformation. Numerically it has been found that for parabolic slip profile, the displacement in magnitude for isotropic elastic medium is greater than that for an orthotropic elastic half-space, but, in case of linear slip, the displacements in magnitude for an orthotropic medium is greater than that for the isotropic medium.

Keywords. Static-deformation; strike-slip line fault; non-uniform slip; orthotropic half-space; rigid boundary.

1. Introduction

Sometimes the cracks are tiny, as thin as hair, with barely noticeable movement between the rock layers. But faults can also be hundreds of miles long, such as the San Andreas Fault in California and the Anatolian Fault in Turkey, both of which are visible from space, so a two-dimensional approximation may be used.

Faults are fractures in Earth's crust where rocks on either side of the crack have slid past each other. To study the effect of faulting at a material discontinuity, many investigators considered the two half-space model. Strike-slip faults are with very little vertical component of motion, i.e., the slip vector is nearly parallel to the strike direction. Strike-slip faults are typically steep or vertical and in Andersonian fault theory, associated with a stress regime where both maximum and minimum stresses are near horizontal. Many strike-slip faults are idealised as being vertical cuts going, presumably, all the way to the core-mantle boundary. In reality, the geometry of apparently vertical strike-slip faults is quite variable with depth. Elastic deformability combined with sample asymmetry, i.e., the mechanical environment of all points on the surface are not identical and can cause non-uniform slip when there is a uniform change in shear stress. Uniform slip could be unstable to small spatial perturbations, thus leading to spatially non-uniform slip (Ruina *et al.* 1986).

For dislocation theory, several studies deal with the mathematical treatment of static elastic residual fields given by Steketee (1958a, b), Chinnery (1961, 1963), Maruyama (1964, 1966) and Press (1965). The static deformation of a semi-infinite elastic isotropic elastic medium due to a very long strike-slip and dip-slip fault has been studied by many researchers, e.g., Kasahara (1964), Rybicki (1971, 1973, 1978, 1986), Savage (1980) and Mavko (1981). However, most of these studies assumed uniform slip on a fault. The assumption of uniform slip makes the edges of the fault plane singular where the displacement is indeterminate and the stress is infinite. For this reason, uniform slip models cannot be used in the vicinity of the fault (near field). There are a number of interesting phenomena that occur near the edge of the fault zone, e.g., vertical movements associated with strike-slip faulting. In order to study these phenomena, it is necessary to consider models of earthquake faulting with non-uniform slip on a fault. In the variable slip models, the amount of slip in a given place and the length of rupture may vary from earthquake to earthquake.

The Nankaido earthquake (1707) demonstrates that the slip in a given place may vary significantly between earthquakes, suggesting the variable slip model. Starr (1928) proposed a two-dimensional elliptical crack model in an infinite medium. Yang and Toksöz (1981) used finite-element method to study the trapezoidal type non-uniform slip on a strike-slip fault in an isotropic elastic half-space. Wang and Wu (1983) obtained closed-form analytical solution for displacement and stress fields due to a non-uniform slip along a strike-slip fault for the same model. Singh *et al.* (1994) obtained closed-form analytical expressions for displacements due to non-uniform slip on a long vertical strike-slip and dip-slip faults in a uniform isotropic elastic half-space. Ghosh *et al.* (1992) discussed about two interacting creeping vertical surface-breaking strike-slip faults in a two-layered model of lithosphere. The results were obtained for creeping and surface breaking long strike-slip fault inclined to the vertical in a viscoelastic half space by Sen *et al.* (1993), Sen and Debnath (2012). Madan *et al.* (2005) obtained static deformation field due to non-uniform slip (parabolic, linear, cubic and elliptic) on a long vertical strike-slip fault in an orthotropic elastic half-space. Two interacting creeping vertical rectangular strike-slip faults in a viscoelastic half-space model of the lithosphere are studied by Debnath *et al.* (2012, 2013).

The upper part of the Earth is anisotropic (Dziewonski and Anderson 1981) and have at least one plane of symmetry (i.e., elastic properties of media have reflection symmetry). A medium having three planes of symmetry is termed as orthorhombic and a large part of our earth is recognised as having orthorhombic symmetry. The orthorhombic symmetry of upper mantle is believed to be caused by orthorhombic crystals of olivine relative to spreading centres (Hess 1964). When one of the planes of symmetry in an orthorhombic symmetry is horizontal, the symmetry is termed as orthotropic (Crampin 1989). Moreover, the orientation of stress in the crust of the earth is usually orthotropic; most symmetry systems in the Earth's crust also have orthotropic orientations. The orthotropic symmetry is also exhibited by olivine and barytes, the principal rock-forming minerals of deep crust and upper mantle.

Garg *et al.* (1996) obtained the representation of seismic sources causing antiplane strain deformation of an orthotropic medium. Garg *et al.* (2003) used an eigen value approach to study the plane strain problem of an infinite orthotropic elastic-medium due to two-dimensional sources.

If we take an elastic half-space (medium 1 with rigidity μ_1) in contact with another elastic half-space (medium 2 with rigidity $r\mu_2$) and if $m = (\mu_1/\mu_2)$, then the two particular cases of special interest are for $m = 0$ and $m \to \infty$. In case $m = 0$, we have an elastic half-space with free boundary. On the other hand, when $m \to \infty$, we have the case an elastic half-space with a rigid boundary. We consider the model consisting of a strike fault in an orthotropic half-space in contact with a rigid half-space. Singh *et al.* (2011) obtained analytical expressions for stresses at an arbitrary point of homogenous, isotropic perfectly elastic half-space with rigid boundary caused by a long tensile fault of finite width. Malik *et al.* (2013) obtained analytical expressions for stresses and displacements at an arbitrary point of homogeneous, isotropic perfectly elastic half-space with rigid boundary caused by a long strike-slip line source. Sahrawat *et al.* (2014) derived the displacements and stresses in a uniform half-space with rigid boundary due to a strike slip fault of finite width. So, it is very interesting to consider the model consisting of an orthotropic half-space with rigid boundary.

In the present problem, we consider a model that consists of a strike-slip fault of finite width in a homogeneous, orthotropic, perfectly elastic half-space in contact with a rigid half-space. This model is useful when the medium on the other side of the material discontinuity is very hard. This paper is a continuation of the paper by Sahrawat *et al.* (2014), in the sense that we have taken the slip as non-uniform instead of uniform slip, and is generalised in the sense that medium of the present paper is orthotropic having rigid boundary which is better approximation than isotropic case. The variations of the displacement with distance from the fault due to various slip profiles have been studied to examine the effect of anisotropy on the deformation. Numerically it has been found that for parabolic slip profile, the surface displacements in magnitude for isotropic elastic medium is greater than that for an orthotropic elastic half-space, but, in case of linear slip, the displacements in magnitude for an orthotropic medium is greater than that for the isotropic medium.

2. Theory

The equations of equilibrium in the absence of body forces, in the Cartesian co-ordinates system $(x, y, z) = (x_1, x_2, x_3)$, are given by:

$$p_{ij,j} = 0, \quad i = (1, 2, 3) \tag{1}$$

where p_{ij} are the components of stress-tensor, and

$$p_{ij,j} \equiv \frac{\partial}{\partial x_j} p_{ij}.$$

Let u_1, u_2, u_3 denote the displacement components. The strain-displacement relations are given by:

$$e_{ij} = \frac{1}{2}\left(u_{i,j} + u_{j,i}\right), \quad (1 \leq i, j \leq 3) \tag{2}$$

where e_{ij} are the components of strain-tensor.

For an orthotropic elastic half-space, with co-ordinate planes coinciding with the axis of symmetry and one plane of symmetry being horizontal, then stress-strain relation in matrix form is

$$\begin{bmatrix} p_{11} \\ p_{22} \\ p_{33} \\ p_{23} \\ p_{31} \\ p_{12} \end{bmatrix} = \begin{bmatrix} c_{11} & c_{12} & c_{13} & 0 & 0 & 0 \\ c_{12} & c_{22} & c_{23} & 0 & 0 & 0 \\ c_{13} & c_{23} & c_{33} & 0 & 0 & 0 \\ 0 & 0 & 0 & c_{44} & 0 & 0 \\ 0 & 0 & 0 & 0 & c_{55} & 0 \\ 0 & 0 & 0 & 0 & 0 & c_{66} \end{bmatrix} \begin{bmatrix} e_{11} \\ e_{22} \\ e_{33} \\ 2e_{23} \\ 2e_{31} \\ 2e_{12} \end{bmatrix} \tag{3}$$

where c_{ij} are elastic constants of the orthotropic medium.

A transversely isotropic elastic medium, with x_3-axis coinciding with the axis of symmetry, is a particular case of an orthotropic elastic medium for which

$$c_{22} = c_{11}, \quad c_{23} = c_{13},$$
$$c_{55} = c_{44}, \quad c_{66} = \frac{1}{2}(c_{11} - c_{12}). \tag{4}$$

The number of independent elastic constants reduces from nine to five and when the medium is isotropic, then elastic constants reduces from five to two as:

$$c_{11} = c_{22} = c_{33} = \lambda + 2\mu,$$
$$c_{12} = c_{13} = c_{23} = \lambda,$$
$$c_{44} = c_{55} = c_{66} = \mu \tag{5}$$

where λ and μ are the Lame's constants.

Here, we consider the anti-strain problem in which the displacement vector is parallel to x_1-axis which is taken to be horizontal and $\partial/\partial x_1 \equiv 0$. Also, consider x_3-axis vertically downwards. In this problem, $u_1 = u_1(x_2, x_3)$ is the only non-zero component of the displacement vector which is perpendicular to the x_2x_3-plane of elastic symmetry. The non-zero stresses can be written as:

$$p_{12} = c\alpha^2 \frac{\partial u_1}{\partial x_2}, \quad p_{13} = c\frac{\partial u_1}{\partial x_3}, \tag{6}$$

where

$$c_{66} = c\alpha^2, \quad c = c_{55}. \tag{7}$$

The values of constants α and c depend upon the elastic constants c_{66} and c_{55}. We assume that α and c are positive real numbers. In case of isotropic elastic medium, $c = \mu$ and $\alpha = 1$.

The equilibrium equation (1) is identically satisfied for the anti-plane deformation and reduces to

$$\frac{\partial^2 u_1}{\partial x_2^2} + \frac{1}{\alpha^2}\frac{\partial^2 u_1}{\partial x_3^2} = 0. \tag{8}$$

We assume that a line-source, parallel to x_1-axis, intersects the x_2x_3-plane of elastic symmetry at the point $\mathrm{P}(0, y_3)$. The displacement u_0, parallel to x_1-axis, due to a line source in an unbounded orthotropic elastic medium is in the following integral form:

$$u_0 = \int_0^\infty \left[A_0 \sin k\, x_2 + B_0 \cos k\, x_2\right] e^{-k\alpha|x_3 - y_3|} dk, \tag{9}$$

where the source co-efficients A_0, B_0 and α are independent of k. Garg *et al.* (1996) obtained these source co-efficients for the single couple (12) and (13) given in Appendix 1.

For a line source parallel to the x_1-axis acting at the point P$(0, y_3)$ in the orthotropic half-space, displacement is given by

$$u_1 = u_0 + \int_0^\infty \left[A \sin kx_2 + B \cos k\, x_2\right] e^{-k\alpha x_3} dk, \tag{10}$$

where A and B are unknown functions of k to be determined from the boundary conditions.

We assume that the surface of the half-space $x_3 \geq 0$ is with rigid boundary. Therefore, the boundary condition is

$$u_1 = 0 \quad \text{at } x_3 = 0. \tag{11}$$

It is noticed from Appendix 1 that A_0 and B_0 have different values for $x_3 < y_3$ and $x_3 > y_3$. Let A^- and B^- be respectively, the values of A_0 and B_0 for $x_3 < y_3$. From equations (10) and (11), we get:

$$A = -A^- e^{-k\alpha y_3}, \quad B = -B^- e^{-k\alpha y_3}. \tag{12}$$

Using the values of A and B in equation (10), we get displacement at any point of orthotropic half-space.

$$u_1 = \int_0^\infty \Big[(A_0 \sin kx_2 + B_0 \cos kx_2) e^{-k\alpha|x_3 - y_3|} - (A^- \sin kx_2 + B^- \cos kx_2) e^{-k\alpha|x_3 + y_3|}\Big] dk. \tag{13}$$

Evaluating the integrals by using standard integral transform, we obtain the displacement as:

$$u_1 = A_0 \frac{x_2}{R^2} - A^- \frac{x_2}{S^2} + B_0 \frac{\alpha\,|x_3 - y_3|}{R^2} - B^- \frac{\alpha\,(x_3 + y_3)}{S^2} \tag{14}$$

where

$$R^2 = x_2^2 + \alpha^2 (x_3 - y_3)^2, \quad S^2 = x_2^2 + \alpha^2 (x_3 + y_3)^2.$$

3. Inclined strike-slip dislocation

The displacement field due to a long inclined strike-slip line dislocation of arbitrary orientation can be expressed as (Maruyama 1966)

$$u_1 = \int \Delta u_1 G^1_{1k}\, n_k ds, \quad (k = 2, 3). \tag{15}$$

Here line integral is over the width of the fault, Δu_1 is the discontinuity of displacement vector in x_1-direction. n_k is the unit normal to the fault of length L and the Green's functions are given by (Maruyama 1966)

$$G^1_{12} = c_{66} \frac{\partial u'}{\partial x_2}, \quad G^1_{13} = c_{55} \frac{\partial u'}{\partial x_3},$$

where u' is the displacement due to a concentrated line force of unit magnitude, per unit length, acting in x_1-direction given by

$$u' = \frac{F}{2\pi c\alpha} \int_0^\infty \frac{1}{k} \cos kx_2\, e^{-k\alpha(x_3 - y_3)} dk.$$

Let $\Delta u_1 = b$.

Writing $n_2 = -\sin\delta$, $n_3 = \cos\delta$, where δ is the dip of the fault (see figure 1a), equation (15) becomes

$$u_1 = \int b(G^1_{13} \cos\delta - G^1_{12} \sin\delta) ds. \tag{16}$$

The Green's function G^1_{12} (corresponds to a long vertical right-lateral strike-slip fault ($\delta = 90°$)) represents dimensionless displacement in x_1-direction at P(x_2, x_3) due to a single couple (12) at $(0, y_3)$. Similarly, the Green's function G^1_{13}(corresponds to a long horizontal strike-slip fault ($\delta = 0°$)) represents dimensionless displacement in x_1-direction at P(x_2, x_3) due to a single couple (13) at $(0, y_3)$.

Therefore, the deformation u_1 at any point of an elastic medium due to an inclined strike slip line source with arbitrary dip will be

$$u_1 = \int \cos\delta\,(\text{displacement due to horizontal strike-slip}) + \sin\delta\,(\text{displacement due to vertical strike-slip}). \tag{17}$$

3.1 *Vertical strike-slip fault*

Suppose we consider the vertical strike-slip fault of infinite length ($-\infty < x_1 < \infty$) and of finite width ($0 \leq x_3 \leq L$) situated on the x_3-axis which is taken vertically downwards (figure 1b), the single couple (12) of moment F_{12} is equivalent to a vertical strike-slip line source such that

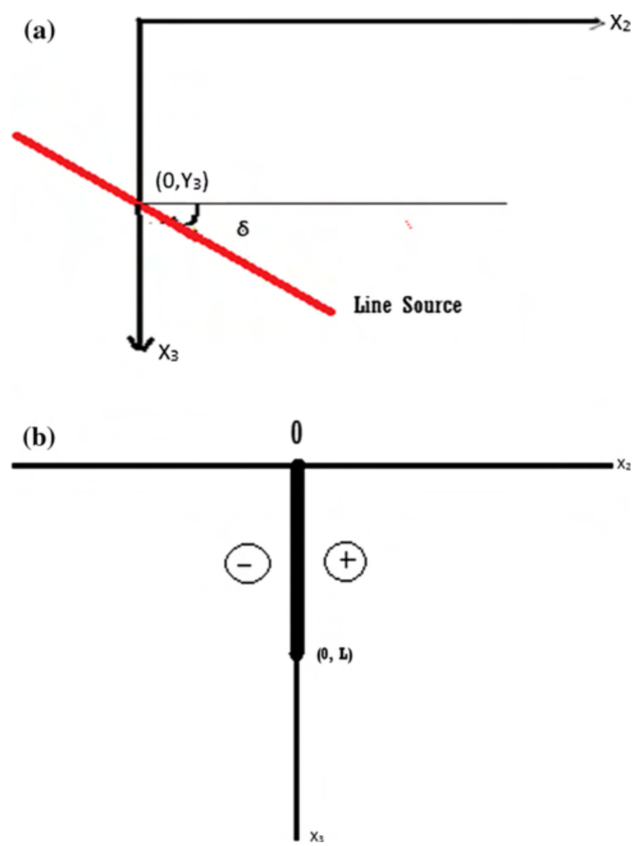

Figure 1. (**a**) An inclined strike-slip line source lying in an orthotropic half-space ($x_3 \geq 0$) with rigid boundary acting at the point $(0, y_3)$. (**b**) Shows the vertical long strike-slip fault in an orthotropic half-space model $x_3 \geq 0, (+)$ and $(-)$ indicate the displacements in the positive x_1-direction and negative x_1-direction, respectively.

$$F_{12} = -c\alpha^2 b\, ds, \tag{18}$$

where b is the slip on the fault which is non-uniform in general and ds is the width of source. Therefore, from Appendix 1, the source co-efficients for a vertical strike-slip are given by

$$A_0 = A^- = \frac{F_{12}}{2\pi c\alpha} = \frac{-\alpha b ds}{2\pi},$$
$$B_0 = B^- = 0. \tag{19}$$

On using these values of the source coefficients from equation (19) into equation (14), the displacement for a vertical strike-slip line source is found to be:

$$u_1 = -\frac{\alpha b ds}{2\pi}\left[\frac{x_2}{R^2} - \frac{x_2}{S^2}\right]. \tag{20}$$

Now, we will discuss the cases on the slip vector $b(s)$ as this leads to singularity in fault plane if we consider a uniform slip.

3.1.1 *Uniform slip*

In this case $b(s) = b_0$, and since we have taken the source of finite width as L by taking the variable s instead of y_3 and integrating the displacement given by equation (20), over the width of the fault $0 \leq s \leq L$, we get the displacement at any point (x_2, x_3) of an orthotropic half-space having rigid boundary due to uniform slip on the fault of width L.

$$u_1 = -\frac{b_0}{2\pi}\left[\tan^{-1}\frac{\alpha(L - x_3)}{x_2} - \tan^{-1}\frac{\alpha(L + x_3)}{x_2} + 2\tan^{-1}\frac{\alpha x_3}{x_2}\right]. \tag{21}$$

3.1.2 *Parabolic slip*

In this case, the slip on the surface breaking fault vary as:

$$b(s) = b_0\left(1 - \frac{s^2}{L^2}\right), \quad (0 \leq s \leq L).$$

Again, using value of b in equation (20) and integrating over width of the fault, we get the displacement in orthotropic half-space having rigid boundary for parabolic slip on the fault

$$u_1 = -\frac{b_0}{2\pi\alpha}\left[\alpha\left(1 - \frac{x_3^2}{L^2} + \frac{x_2^2}{\alpha^2 L^2}\right) \times \left\{\tan^{-1}\frac{\alpha(L - x_3)}{x_2} - \tan^{-1}\frac{\alpha(L + x_3)}{x_2} + 2\tan^{-1}\frac{\alpha x_3}{x_2}\right\} - \frac{2x_2 x_3}{L^2}\log\left(\frac{AB}{C^2}\right)\right]. \tag{22}$$

3.1.3 *Linear slip*

Here, the slip on the fault vary according to the law

$$b(s) = b_0\left(1 - \frac{s}{L}\right), \quad (0 \leq s \leq L).$$

From equation (20), the displacement at any point of an orthotropic half-space having rigid boundary is given as:

$$u_1 = -\frac{b_0}{2\pi\alpha}\left[\frac{x_2}{L}\log\left(\frac{B}{A}\right) + \alpha\left(1 - \frac{x_3}{L}\right)\tan^{-1}\frac{\alpha(L - x_3)}{x_2}\right.$$

$$-\alpha\left(1+\frac{x_3}{L}\right)\tan^{-1}\frac{\alpha(L+x_3)}{x_2}$$
$$\left.+2\tan^{-1}\frac{\alpha x_3}{x_2}\right], \qquad (23)$$

where

$$A^2 = x_2^2 + \alpha^2 (L - x_3)^2,$$
$$B^2 = x_2^2 + \alpha^2 (L + x_3)^2,$$
$$C^2 = x_2^2 + \alpha^2 x_3^2.$$

The expressions for stresses for different slip profiles are given in Appendix 2.

3.1.4 *Elliptic slip*

$$b(s) = b_0\left(1 - \frac{s^2}{L^2}\right)^{1/2}, \quad (0 \le s \le L).$$

Using value of b for elliptic slip in equation (20) and integrating over width of fault, explicit integrals could not be found in the medium. Also surface displacement ($x_3 = 0$) vanishes due to rigid boundary which is clear from the equation (20), when we put $x_3 = 0$ in equation (20), the displacement vanishes.

3.1.5 *Cubic slip*

$$b(s) = b_0\left(1 - \frac{s^2}{L^2}\right)^{3/2}, \quad (0 \le s \le L).$$

Using value of b for cubic slip in equation (20) and integrating over width of fault, explicit integrals could not be found in the medium. Also, surface displacement ($x_3 = 0$) vanishes due to rigid boundary which is clear from the equation (20); when we put $x_3 = 0$ in equation (20), displacement vanishes.

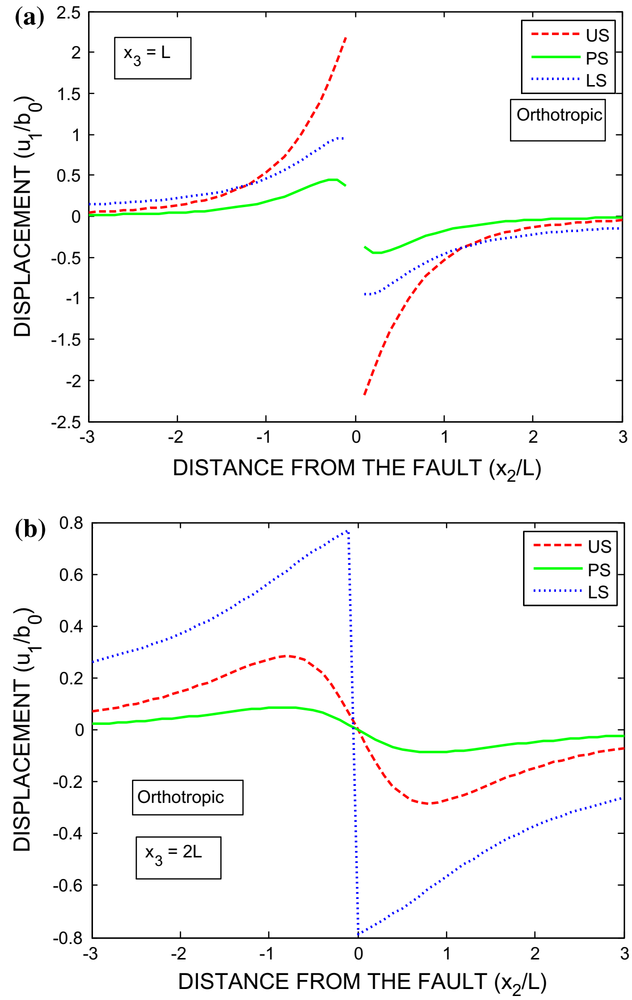

Figure 2. Variation of displacement (u_1/b_0) with distance from the fault (x_2/L) for different slip profiles for an orthotropic elastic medium with rigid boundary at (**a**) $x_3 = L$ and (**b**) $x_3 = 2L$.

4. Numerical results and discussion

In the present study, we compare the displacement field due to non-uniform slip along a strike slip fault lying in an orthotropic elastic medium having rigid boundary with the corresponding displacement field due to uniform slip along a strike slip fault in the same model.

For all slip profiles, the slip decreases from the interface b_0 and the fault width L to be the same for all the cases, the source potency $\int_0^L b(h)\,dh$ per unit length of the fault is different for different profiles. It is not justified to compare the displacement field of different source potencies. Therefore, equality in source potency must be assured. To get it, we adjust the fault width, keeping the value of slip at the interface to be same. This gives the relation

$$L_1 = \frac{1}{2}L_2 = \frac{2}{3}L_3 = \frac{\pi}{4}L_4 = \frac{3\pi}{16}L_5 = L, \quad (24)$$

where L_1 is the fault width for uniform slip and L_2, L_3, L_4, L_5 are the fault widths for linear, parabolic, elliptic and cubic profiles considered, respectively.

We measure the displacements in units of fault width L for uniform slip and the quantities x_2/L and x_3/L for non-uniform slip cases to be suitably modified in accordance with relation (24).

Figure 2(a–b) displays the variation of displacement (u_1/b_0) with distance from the fault (x_2/L) for different slip profiles for an orthotropic elastic medium with rigid boundary at (a) $x_3 = L$,

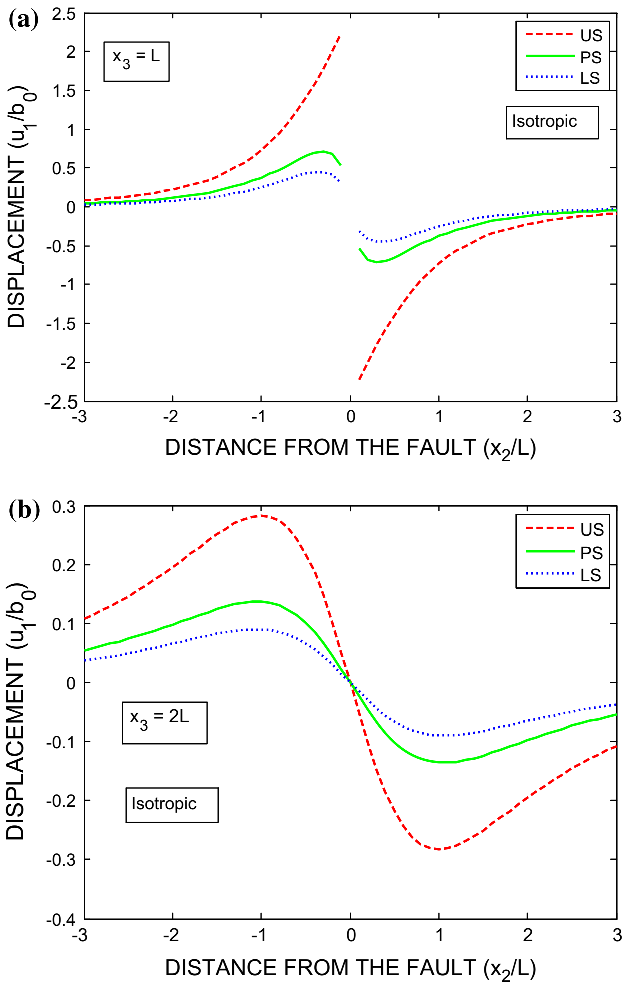

Figure 3. Variation of displacement (u_1/b_0) with distance from the fault (x_2/L) for different slip profiles for an isotropic elastic medium with rigid boundary at (**a**) $x_3 = L$ and (**b**) $x_3 = 2L$.

(b) $x_3 = 2L$. The displacement varies significantly near the edge of the fault. For uniform slip, the displacement is indeterminate near the edge of the fault plane, but there is no singularity for parabolic and linear slip profiles. The same behaviour is observed in case of an isotropic elastic medium with rigid boundary in figure 3(a–b). Also, the displacement is anti-symmetric about $x_2 = 0$ and near the edge of the fault, displacement function is discontinuous for all slip profiles.

Here, we will examine the effect of the anisotropy on deformation due to non-uniform slip along a vertical strike-slip fault of width L. For this reason, we compare the results for an orthotropic elastic medium having rigid boundary with isotropic elastic medium having rigid boundary. For an orthotropic elastic medium, we assume $\alpha = 0.80$ and for an isotropic medium, $\alpha = 1$.

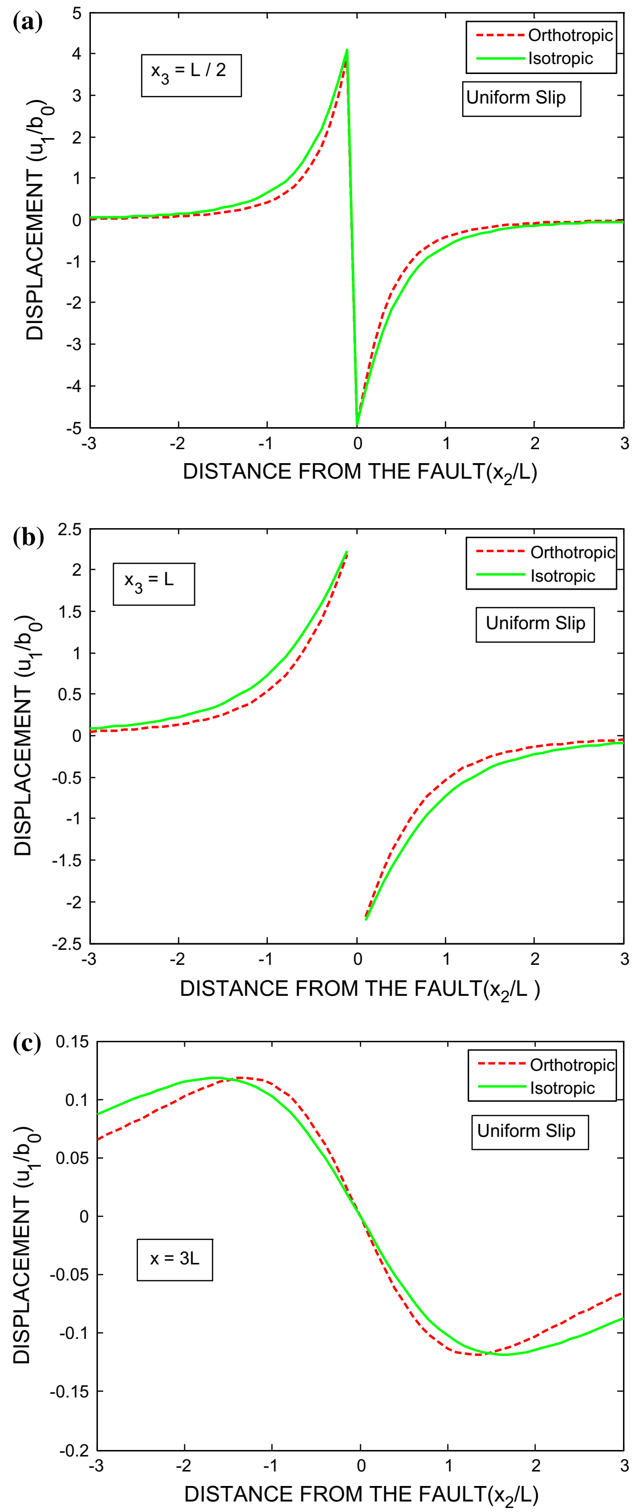

Figure 4. Variation of horizontal displacement (u_1/b_0) with distance from the fault (x_2/L) for uniform slip for an orthotropic elastic medium and isotropic elastic medium with rigid boundary at (**a**) $x_3 = L/2$, (**b**) $x_3 = L$ and (**c**) $x_3 = 3L$.

Figure 4 depicts the variation of displacement along (a) the mid-point of the fault, (b) upper edge of the fault, and (c) far from the fault for both

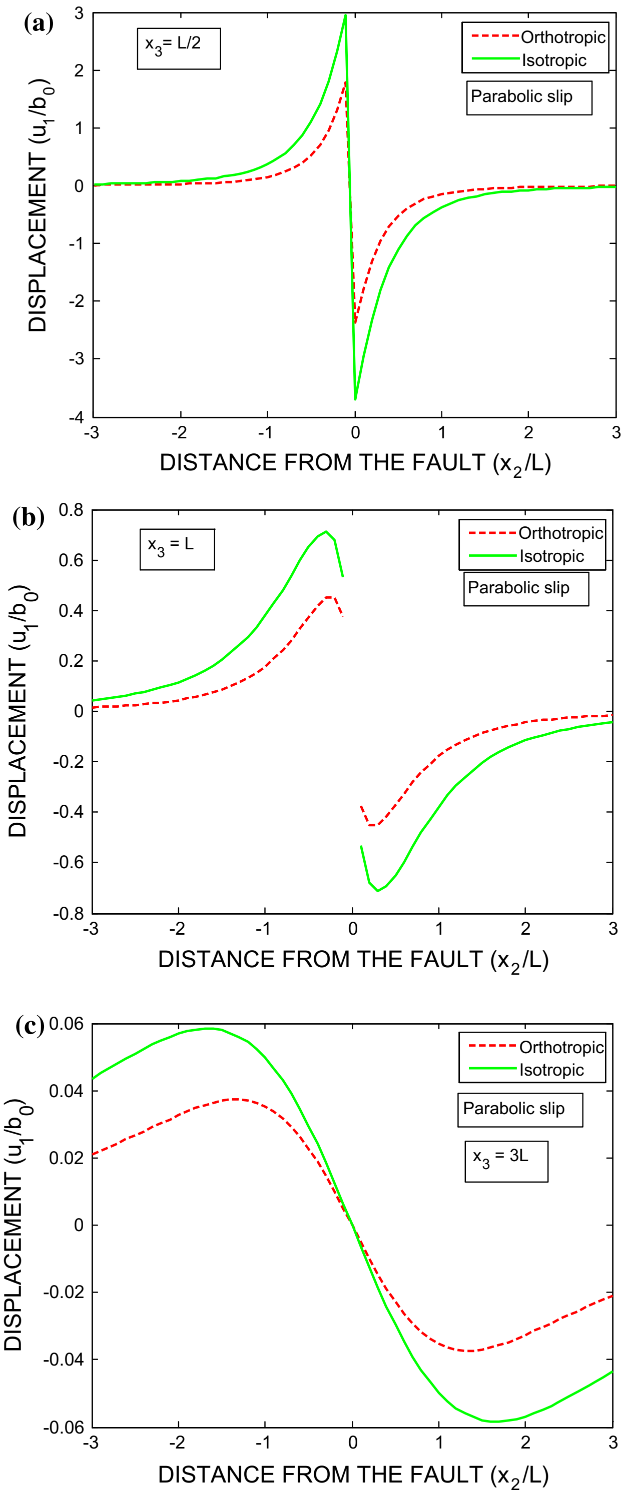

Figure 5. Variation of horizontal displacement (u_1/b_0) with distance from the fault (x_2/L) for parabolic slip for an orthotropic elastic medium and isotropic elastic medium with rigid boundary at (**a**) $x_3 = L/2$, (**b**) $x_3 = L$ and (**c**) $x_3 = 3L$.

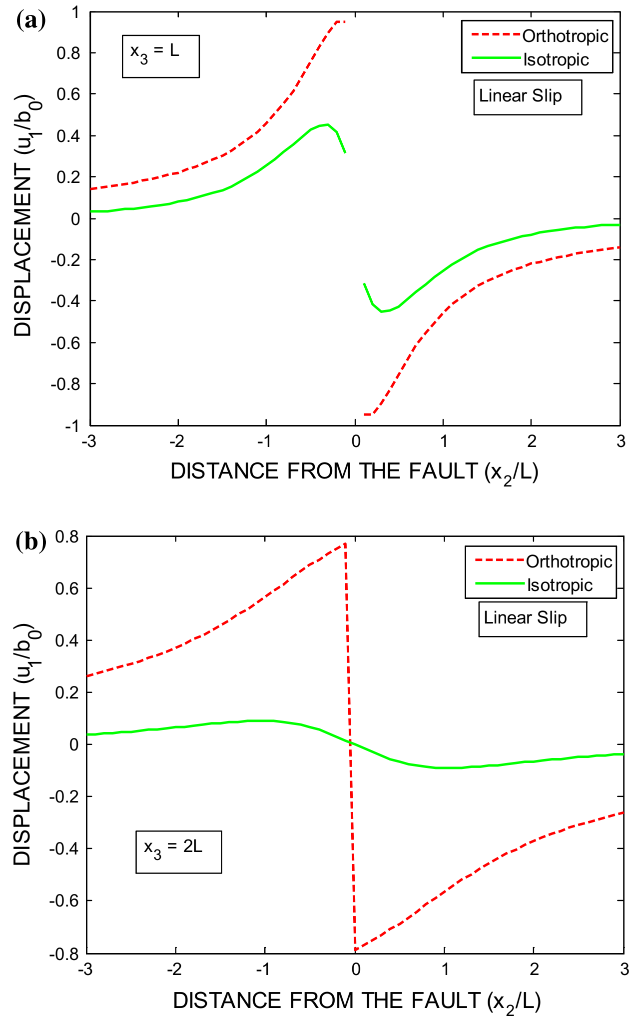

Figure 6. Variation of horizontal displacement (u_1/b_0) with distance from the fault (x_2/L) for linear slip for an orthotropic elastic medium and isotropic elastic medium with rigid boundary at (**a**) $x_3 = L$ and (**b**) $x_3 = 2L$.

isotropic and orthotropic half-space having rigid boundary. As we go vertically far from the fault, the displacement decreases. From figure 4(a–c), it is obvious that the uniform slip cannot be used near the edge of the fault. But figures 5(a–c) and 6(a–b) show that near field deformation can be determined for parabolic and linear slip. Figures 4 and 5 show that for uniform and parabolic slip, the surface displacements in ma gnitude for isotropic medium is greater than that of orthotropic medium, while figure 6 shows that the displacements in magnitude, in case of linear slip, for an orthotropic medium with rigid boundary is greater than that for the isotropic medium with rigid boundary. The assumption of uniform slip makes the edges of the fault plane singular where the displacement is indeterminate and the stress is infinite.

From these figures it is found that, in case of parabolic, linear slips, as we move away from the fault horizontally, the difference between the displacement for an orthotropic and isotropic medium having rigid boundary decreases.

5. Conclusion

In the present problem, we have derived the closed form expressions for displacements and stresses at any point of a homogeneous, orthotropic, perfectly elastic half-space in contact with a rigid half-space due to non-uniform slip-profiles – linear and parabolic along a very long strike-slip fault. This paper is a continuation of the paper by Sahrawat *et al.* (2014), in the sense that we have taken the slip as non-uniform instead of uniform slip, and is generalised in the sense that medium of the present paper is orthotropic having rigid boundary which is better approximation than isotropic case. The variations of the displacement with distance from the fault due to various slip profiles have been studied to examine the effect of anisotropy on the deformation. Numerically it has been found that for parabolic slip profile, the surface displacements in magnitude for isotropic elastic medium is greater than that for an orthotropic elastic half-space, but, in case of linear slip, the displacements in magnitude for an orthotropic medium is greater than that for the isotropic medium.

The analytical solution obtained here is useful in modelling the lithospheric deformation associated with vertical strike slip faulting in the earth. In the field, people have frequently encountered approximately equal spacing between the faults, i.e., uniform slip on the fault. While for normal faults and reverse faults it may have to do with the dominant wavelength of folding, the assumption of uniform slip makes the edges of the fault plane singular where the displacement is indeterminate and the stress is infinite. For this reason, uniform slip models cannot be used in the near field. The present paper may find applications in modelling crustal deformation due to non-uniform long vertical strike-slip faults.

This model is also useful when the medium on the other side of the material discontinuity is very hard. High-rigidity layers are generally present at depth below a volcanic edifice, covered by much softer volcanic-sedimentary layers composed of a mixture of ash, mud and lava (Bonafede and Rivalta 1999).

Acknowledgements

Yogita Godara (SRF) is grateful to the Council of Scientific and Industrial Research, New Delhi for the financial support. Authors thank the referees for their useful suggestions which led to an improvement in the presentation of the paper.

Appendix 1

For the single couple (12)

$$A_0 = \frac{F_{12}}{2\pi c\alpha}, \quad B_0 = 0.$$

For the single couple (13)

$$A_0 = 0, \quad B_0 = \pm\frac{F_{13}}{2\pi c},$$

where the upper sign is for $x_3 > y_3$ and the lower sign is for $x_3 < y_3$.

Appendix 2

Stresses in case of uniform slip

$$P_{12} = \frac{c\alpha^3 b_0}{2\pi}\left[\frac{L-x_3}{A^2} - \frac{L+x_3}{B^2} + \frac{2x_3}{C^2}\right],$$
$$P_{13} = \frac{c\alpha b_0}{2\pi}\left[\frac{x_2}{A^2} + \frac{x_2}{B^2} - \frac{2x_3}{C^2}\right].$$

Stresses in case of parabolic slip

$$\begin{aligned} P_{12} = -\frac{c\alpha b_0}{2\pi L}\Bigg[\frac{2x_2}{\alpha L}\Bigg\{&\tan^{-1}\frac{\alpha(L-x_3)}{x_2} \\ &-\tan^{-1}\frac{\alpha(L+x_3)}{x_2} + 2\tan^{-1}\frac{\alpha x_3}{x_2}\Bigg\} \\ &-\alpha\left(L - \frac{x_3^2}{L} + \frac{x_2^2}{\alpha^2 L}\right)\Bigg\{\frac{\alpha(L-x_3)}{A^2} \\ &-\frac{\alpha(L+x_3)}{B^2} + \frac{2\alpha x_3}{C^2}\Bigg\} - \frac{2x_3}{L}\log\left(\frac{AB}{C^2}\right) \\ &-\frac{2x_2^2 x_3}{L}\left\{\frac{1}{A^2} + \frac{1}{B^2} - \frac{2}{C^2}\right\}\Bigg] \end{aligned}$$

$$\begin{aligned} P_{13} = \frac{cb_0}{2\pi\alpha L}\Bigg[\frac{2\alpha x_3}{L}\Bigg\{&\tan^{-1}\frac{\alpha(L-x_3)}{x_2} \\ &-\tan^{-1}\frac{\alpha(L+x_3)}{x_2} + 2\tan^{-1}\frac{\alpha x_3}{x_2}\Bigg\} \\ &+\alpha^2 x_2\left(L - \frac{x_3^2}{L} + \frac{x_2^2}{\alpha^2 L}\right)\left\{\frac{1}{A^2} + \frac{1}{B^2} - \frac{2}{C^2}\right\} \end{aligned}$$

$$+\frac{2x_2}{L}\log\left(\frac{AB}{C^2}\right)-\frac{2\alpha^2x_2x_3}{L}$$
$$\times\left\{\frac{L-x_3}{A^2}-\frac{L+x_3}{B^2}+\frac{2x_3}{C^2}\right\}\Bigg]$$

References

Bonafede M and Rivalta E 1999 The tensile dislocation problem in a layered elastic medium; *Geophys. J. Int.* **136** 341–356.

Chinnery M A 1961 The deformation of the ground around surface faults; *Bull. Seismol. Soc. Am.* **61** 355–372.

Chinnery M A 1963 The stress changes that accompany strike-slip faulting; *Bull. Seismol. Soc. Am.* **53** 921–932.

Crampin S 1989 Suggestions for a consistent terminology for seismic anisotropy; *Geophys. Prospect.* **37** 753–770.

Debnath S K and Sen S 2012 Two interacting creeping vertical rectangular strike-slip faults in a viscoelastic half-space model of the lithosphere; *IJSER* **4(6)** 1058–1071.

Debnath S K and Sen S 2013 Pattern of stress-strain accumulation due to a long dip-slip fault movement in a viscoelastic layer over a viscoelastic half-space model of the lithosphere–asthenosphere system; *Int. J. Appl. Mech. Eng.* **18(3)** 653–670.

Dziewonski A M and Anderson D L 1981 Preliminary reference earth model; *Phys. Earth Planet. Int.* **25** 297–356.

Garg N R, Madan D K and Sharma R K 1996 Two-dimensional deformation of an orthotropic elastic medium due to seismic sources; *Phys. Earth Planet. Int.* **94(1)** 43–62.

Garg N R, Kumar R, Goel A and Miglani A 2003 Plane strain deformation of an orthotropic elastic medium using an eigen value approach; *Earth Planet. Space* **55** 3–9.

Ghosh U, Mukhopadhyay A and Sen S 1992 On two interacting creeping vertical surface-breaking strike-slip faults in a two-layered model of lithosphere; *Phys. Earth Planet. Int.* **70** 119–129.

Hess H 1964 Seismic anisotropy of the uppermost mantle under oceans; *Nature* **203** 629–631.

Kasahara K 1960 Static and dynamic characteristics of earthquake faults; *Bull. Earthq. Res. Inst.*, University of Tokyo, pp. 74–75.

Kasahara K 1964 A strike-slip fault buried in a layered medium; *Bull. Earthq. Res. Inst.*, University of Tokyo **42** 609–619.

Madan D K, Singh K, Aggarwal R and Gupta A 2005 Displacements and stresses in anisotropic medium due to non-uniform slip along a very long strike-slip fault; *ISET J. Earthq. Technol.* **42(1)** 1–11.

Malik M, Singh M and Singh J 2013 Static deformation of a uniform half-space with rigid boundary due to a strike slip line source; *IOSR-JM* **5** 30–41.

Maruyama T 1964 Static elastic dislocation in an infinite and semi-infinite medium; *Bull. Earthq. Res. Inst.,* University of Tokyo **42** 289–368.

Maruyama T 1966 On two-dimensional elastic dislocations in an infinite and semi-infinite medium; *Bull. Earthq. Res. Inst.*, University of Tokyo **44** 811–871.

Mavko G M 1981 Mechanics of motion on major faults; *Ann. Rev. Earth Planet. Sci.* **9** 81–111.

Press F 1965 Displacements, strains and tilts at teleseismic distances; *J. Geophys. Res.* **70** 2395–2412.

Ruina A, Katzman Y, Conrad G and Horowitz F G 1986 Some theory and experiments related to frictional behaviour of rocks at low normal stress; *Pure Appl. Geophys.* 1–82.

Rybicki K 1971 The elastic residual field of a very long strike slip fault in the presence of a discontinuity; *Bull. Seismol. Soc. Am.* **61** 79–92.

Rybicki K 1973 Static deformation of a multilayered half-space by a very long strike slip fault; *Pure Appl. Geophys.* **110** 1955–1966.

Rybicki K 1978 Static deformation of a laterally inhomogeneous half-space by a two-dimensional strike-slip fault; *J. Phys. Earth* **26** 351–366.

Rybicki K 1986 Dislocations and their geophysical application; In: *Continuum Theories in Solid Earth Physics*, Elsevier, Amsterdam, The Netherlands, pp. 18–186.

Sahrawat R K, Godara Y and Singh M 2014 Deformation of a uniform half-space with rigid boundary caused by a long inclined strike slip fault of finite width; *IOSR-JM* **10(3)** 100–108

Satake K 1994 Mechanism of the 1992 Nicaragua Tsunami earthquake; *Geophys. Res. Lett.* **21(23)** 2519–2522.

Savage J C 1980 Dislocations in seismology in dislocations in solids; In: *Moving Dislocations* (ed.) F R N Nabarro, North-Holland, Amsterdam, The Netherlands, **3** 251–339.

Sen S, Sarker S and Mukhopadhyay A 1993 A creeping and surface breaking long strike-slip fault inclined to the vertical in a viscoelastic half-space; *Mausam* **44** 365–4, 372–4.

Sen S and Debnath S K 2012 A creeping vertical strike-slip fault of finite length in a viscoelastic half-space model of the lithosphere; *Int. J. Comput.* **2(3)** 687–697.

Singh S J, Punia M and Rani S 1994 Crustal deformation due to non-uniform slip along a long fault; *Geophys. J. Int.* **118** 411–427

Singh J, Malik M and Singh M 2011 Deformation of a uniform half-space with rigid boundary due to long tensile fault; *ISET J. Earthq. Technol.* **48** 1–11.

Starr A T 1928 Slip in a crystal and rupture in a solid due to shear; *Proc. Cambridge Philosophical Soc.* **24** 489–500.

Steketee J A 1958a On Volterra's dislocations in a semi-infinite elastic medium; *Can. J. Phys.* **36** 192–205.

Steketee J A 1958b Some geophysical applications of the elasticity theory of dislocations; *Can. J. Phys.* **36** 1168–1198.

Wang R and Wu H L 1983 Displacement and stress fields due to a non-uniform slip along a strike slip fault; *Pure Appl. Geophys.* **121** 601–609.

Yang M and Toksöz M N 1981 Time dependent deformation and stress relation after strike-slip earthquakes; *J. Geophys. Res.* **86(B4)** 2889–2901.

Corresponding editor: PAWAN DEWANGAN